Electronic Supplementary Material (ESI) for Journal of Materials Chemistry A.

Supporting Information for

Branched Alkyl-chain Engineering of Chlorinated Asymmetrical Acceptors for Improved Organic Photovoltaic Performance

Dandan Li,[a‡] Gang Li,*[a‡] Zhixiang Li,[b] Lingxian Meng,[b] Yan Xu,[a] Guanwei Cui,[a] Yunfei Bai,[a] Xiangjian Wan,*[a] Yongsheng Chen*[a] and Bo Tang*[a]

[a] College of Chemistry, Chemical Engineering and Materials Science, Key Laboratory of Molecular and Nano Probes, Ministry of Education, Collaborative Innovation Center of Functionalized Probes for Chemical Imaging in Universities of Shandong, Institute of Materials and Clean Energy, Shandong Provincial Key Laboratory of Clean Production of Fine Chemicals, Shandong Normal University, Jinan 250014, China. E-mail: ligang@sdnu.educn; tangb@sdnu.edu.cn

[b] The Centre of Nanoscale Science and Technology and Key Laboratory of Functional Polymer Materials, Institute of Polymer Chemistry, College of Chemistry, Nankai University, Tianjin 300071, China E-mail: xjwan@nankai.edu.cn;yschen99@nankai.edu.cn

[‡] These authors contributed equally to this work.

Materials

All solvents and chemicals used were purchased from Energy Chemical, Aladdin, Innochem and SPAKE or other commercial resources and used as received. All reactions were heated by metal sand bath (WATTCAS, LAB-500, http://www.wattcas.com). Toluene and THF were distilled from sodium benzophenone under nitrogen. Anhydrous DMF was distilled from CaH_2. PM6 and IC-2Cl were purchased from Solarmer Materials Inc (Beijing).

Instruments and Measurement

^1H and ^{13}C NMR spectra were recorded on a Bruker AVIII-400M (400 MHz and 100 MHz, respectively) spectrometer at room temperature. ^1H and ^{13}C NMR chemical shifts were determined relative to internal standard TMS at δ 0.0, $CDCl_3$ (δ ^1H, 7.26 ppm; δ ^{13}C, 77.16 ppm). The spectroscopic solvents were purchased from Cambridge Isotope Laboratories. Chemical shifts (δ) are reported in ppm. The following abbreviations are used to explain the multiplicities: s = singlet, d = doublet, t = triplet, q = quartet, m = multiplet, br = broad.

Analytical thin layer chromatography (TLC) was performed on 0.25 mm silica gel 60 F254 plates and viewed by UV light (254 nm). Column chromatographic purification was performed using 100-200 or 200-300 mesh silica gel. Mass spectra were measured on a Bruker Maxis UHR-TOF MS spectrometer. UV-vis absorption spectra were performed with a Beijing Purkinje General Instrument Co. Ltd. TU-1901 spectrophotometer. All steady-state measurements were carried out using a quartz cuvette with a path length of 1 cm. Photoluminescence (PL) quenching experiments were recorded on an Edinburgh Instruments FLS1000 double-monochromator spectrophotometer. Thermogravimetric analysis (TGA) was carried out on a TA Instrument TA Q50 Thermogravimetric Analyzer at a heating rate of 10 ^oC /min up to 800 ^oC.

Solar cell fabrication and characterization

Solar cells were fabricated in a conventional device configuration of ITO/PEDOT: PSS/Active layer/ PNDIT-F_3N/Ag. The ITO-coated glass substrates were cleaned by ultrasonic treatment in detergent, deionized water, acetone, and isopropyl alcohol under ultra-sonication for 15 minutes each and subsequently dried by a nitrogen blow. The glass substrates were treated by UV-Ozone for 15 min before use. PEDOT: PSS (Heraeus Clevios P VP A 4083) layer was spin-cast onto the ITO substrates at 4300 rmp for 30s.After baked at 150 °C for 20 minutes,the substrates were transferred into an argonfilled glove box. The donor:acceptor blends with 1:1 ratio were dissolved in chlorobenzene (the concentration of blend solutions are 20 mg/mL for all blend films), and stirred overnight in a nitrogen-filled glove box. Subsequently, the blend solution was spin-coated to form the active layers with a thickness of 110 nm. Then the substrates were TA treatment at 100 ℃ for 5 min for all acceptors.A thin PNDIT-F_3N layer (10 nm) and Ag layer (100 nm) were sequentially evaporated through a shadow mask under vacuum of 1.5×10^{-4} Pa.

Space charge-limited current (SCLC) device fabrication

The hole and electron mobility were measured using the space charge limited current (SCLC) method, employing a diode configuration of ITO/PEDOT:PSS/active layer/Ag for hole and glass/ITO/ZnO/active layer/Al for electron by taking the dark current density in the range of 0-8 V and fitting the results to a space charge limited form, where SCLC is described by:

$$J = \frac{9\varepsilon_0\varepsilon_r\mu_0(V - V_{\mathrm{bi}})^2}{8L^3}$$

where J is the current density, L is the film thickness of the active layer, μ is the hole or electron mobility, ε_r is the relative dielectric constant of the transport medium, ε_0 is the permittivity of free space (8.85×10^{-12} F m^{-1}), V is the applied voltage to the device and V_{bi} is the built-in voltage due to the relative work function difference of the two electrodes.

Film and Device Characterization

UV-vis spectra were obtained with a Cary 5000 Spectrophotometers. The optimal blend thickness was about 110 nm, measured on a Bruker Dektak XT stylus profilometer. The current density-voltage (J-V) curves of photovoltaic devices were obtained by a Keithley 2400 source-measure unit. The photocurrent was measured under AM 1.5G illumination at 100 mW cm^{-2} irradiation using a SAN-EI XES-70S1 solar simulator, calibrated with a standard Si solar cell.The external quantum efficiency (EQE) spectrum was measured using a QE-R Solar Cell Spectral Response Measurement System (Enli Technology Co., Ltd., Taiwan).

Electrochemical Characterization.

Cyclic voltammogram (CV) was performed with a CHI 660C electrochemical workstation at a scan rate of 100 mV/s. The highest occupied molecular orbital (HOMO) and lowest unoccupied molecular orbital (LUMO) energy levels were calculated from the onset oxidation potential and the onset reduction potential, using the equation $E_{HOMO} = -(4.80+E_{ox}^{onset})$, $E_{LUMO} = -(4.80+E_{re}^{onset})$.

Atomic force microscope (AFM) Characterization

AFM measurements were performed by using a Scanning Probe Microscope-Dimension 3100 in tapping mode. All films were coated on ITO glass substrates.

Grazing incidence wide angle X-ray scattering (GIWAXS) Characterization

The grazing incidence wide angle X-ray scattering (GIWAXS) were conducted at Beijing Synchrotron Radiation Facility (BSRF), Institute of High Energy Physics. All samples were prepared on ZnO-coated Si substrates using the same preparation conditions as for devices. All simples were irradiated at a fixed X-ray incident angle of 0.2° with an exposure time of 1200s.

Synthetic procedures

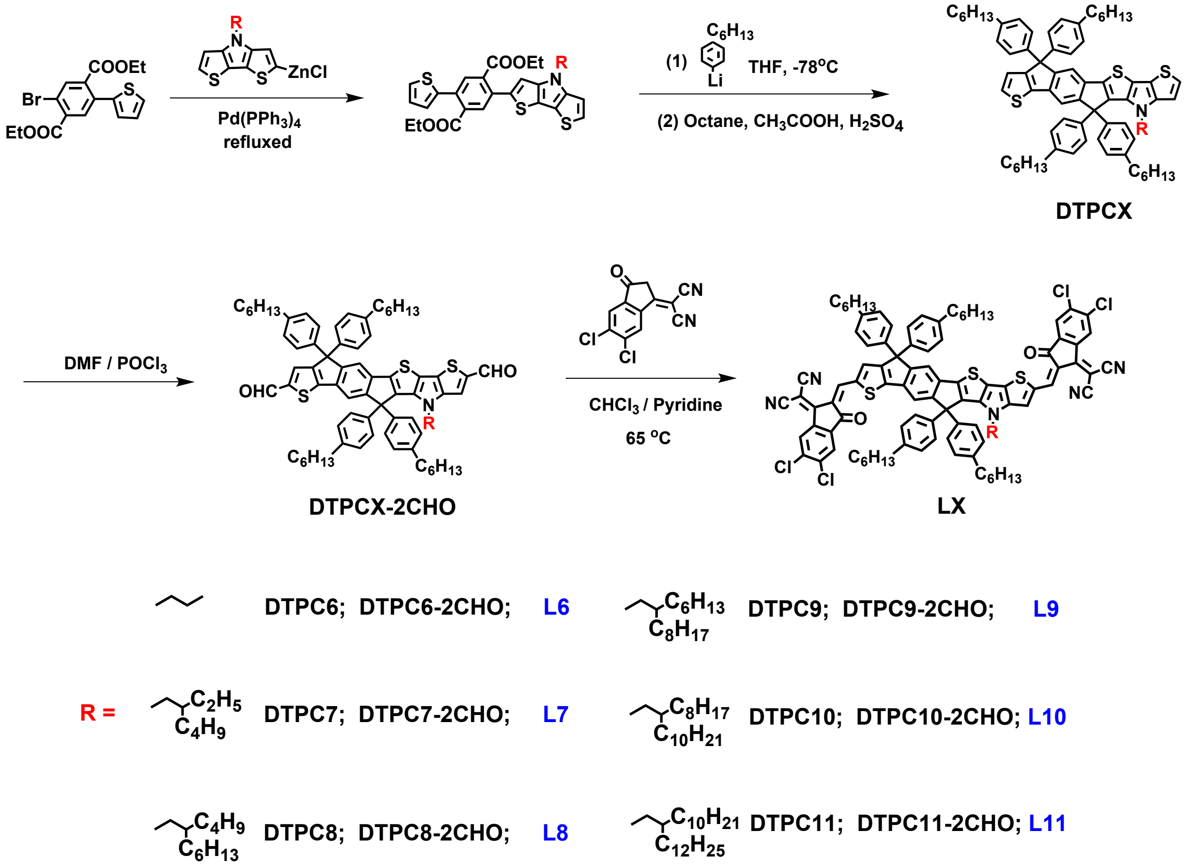

Scheme S1. The synthetic route of six acceptors.

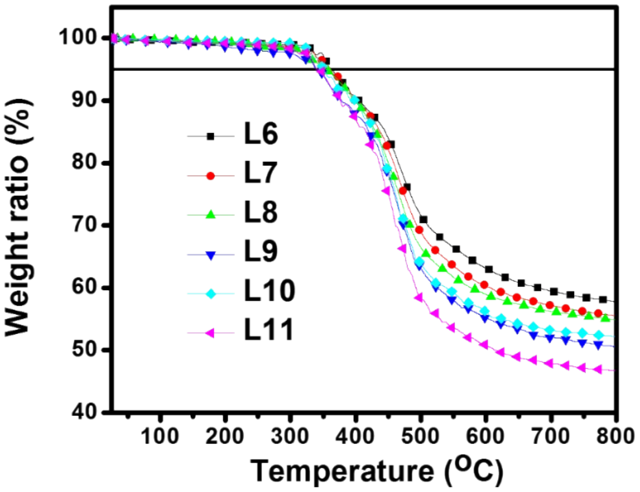

Figure S1. TGA profiles of six acceptors.

Table S1. Basic properties of L6-L11.

Acceptor	$\lambda_{max}$$^{a)}$ (nm)	$\varepsilon_{max}$$^{a)}$ (M^{-1} cm^{-1})	$\lambda_{onset}$$^{a)}$ (nm)	$\lambda^{film}_{max}$$^{b)}$ (nm)	$\lambda^{film}_{onset}$$^{b)}$ (nm)	E_g^{opt} (eV)	HOMO (eV)	LUMO (eV)
L6	748	2.75×10^5	791	804	865	1.43	–5.56	–3.97
L7	748	2.51×10^5	791	806	866	1.43	–5.54	–3.92
L8	748	3.13×10^5	791	805	859	1.43	–5.61	–3.92
L9	748	2.04×10^5	791	807	865	1.43	–5.63	–3.91
L10	748	2.33×10^5	791	805	864	1.43	–5.65	–3.93
L11	748	2.28×10^5	791	805	871	1.42	–5.67	–3.92

a) In a chloroform solution. b) In a neat film.

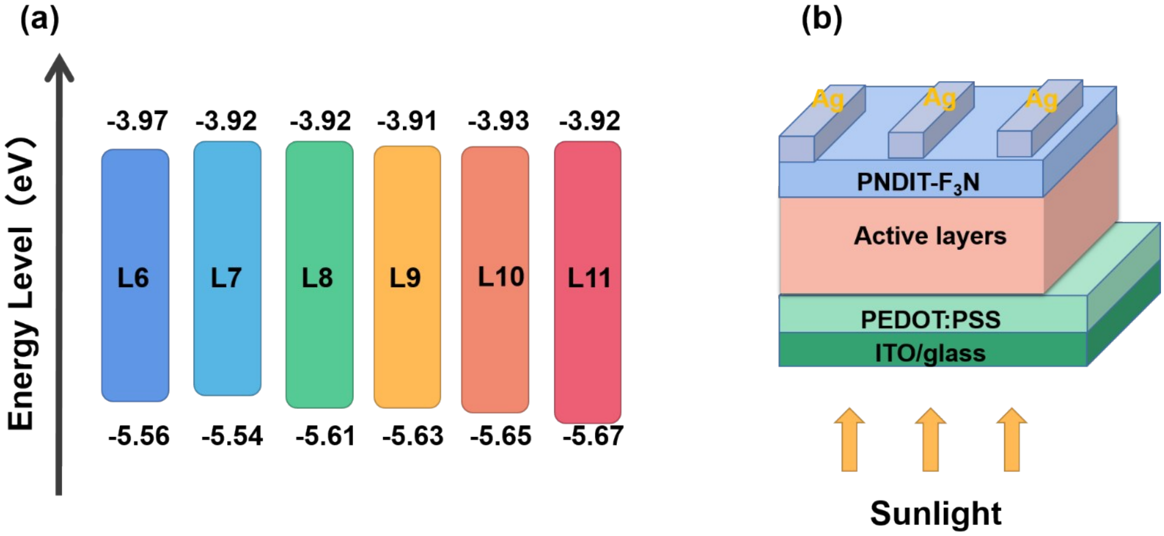

Figure S2. (a) Energy level diagrams for L6-L11.（b）The OSCs devices diagram.

Table S2. Photovoltaic parameters of the OSCs based on PM6:L8 with different D/A weight ratios under the illumination of AM1.5G (100 mA/cm^2).

D:A	V_{oc} (V)	FF	J_{sc} (mA/cm^2)	PCE (%)
0.8:1	0.907	0.653	21.17	12.52
1:1	0.903	0.637	22.17	12.72
1:1.2	0.900	0.637	20.77	11.88
1:1.4	0.894	0.592	22.03	11.63

Table S3. Photovoltaic performance of the solar cells based on PM6:L8 (1:1, w/w) with different thermal annealing (TA) temperature under illumination of AM1.5G (100 mA/cm^2).

TA (°C)	V_{oc} (V)	*FF*	J_{sc} (mA/cm^2)	PCE (%)
80	0.896	0.659	-22.00	12.97
100	0.895	0.675	-22.57	13.62
120	0.887	0.662	-22.35	13.11
140	0.868	0.663	-22.15	12.88

Table S4. Photovoltaic performance of the solar cells based on PM6:L8 (1:1, w/w) with different amounts of DIO additive under illumination of AM1.5G (100 mA/cm^2).

DIO (%)	V_{oc} (V)	*FF*	J_{sc} (mA/cm^2)	PCE (%)
0.5	0.887	0.668	-23.14	13.71
0.7	0.881	0.705	-23.59	14.66
1	0.883	0.684	-22.45	13.67

Table S5. Photovoltaic performance of the solar cells based on PM6:L8 (1:1, w/w) with different donor concentration under illumination of AM 1.5 G, 100 mW cm^{-2}.

Conc. (mg/ml)	V_{oc} (V)	*FF*	J_{sc} (mA/cm^2)	PCE (%)
9	0.867	0.738	21.47	13.83
10	0.864	0.754	23.63	15.40
11	0.871	0.731	21.23	13.62

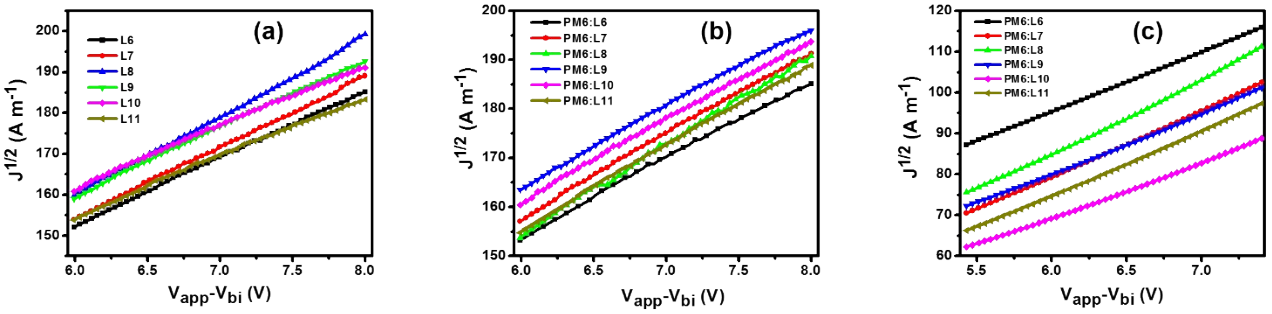

Figure S3. Charge carrier mobility of (a) L6-L11, electron mobility; (b) L6-L11 blended with PM6, electron mobility; (c) L6-L11 blended with PM6, hole mobility.

Table S6. Charge mobilities measured by SCLC method.

Samples	**Electron mobility (cm^2 V^{-1} s^{-1})**	**Hole mobility (cm^2 V^{-1} s^{-1})**	**μ_e/μ_h**
PM6: L6	1.11×10^{-4}	0.892×10^{-4}	1.24
PM6: L7	1.21×10^{-4}	1.06×10^{-4}	1.14
PM6: L8	1.41×10^{-4}	1.38×10^{-4}	1.02
PM6: L9	1.16×10^{-4}	1.01×10^{-4}	1.15

PM6: L10	1.13×10^{-4}	0.914×10^{-4}	1.23
PM6: L11	1.20×10^{-4}	0.994×10^{-4}	1.21
L6	1.14×10^{-4}	-	-
L7	1.25×10^{-4}	-	-
L8	1.54×10^{-4}	-	-
L9	1.16×10^{-4}	-	-
L10	0.931×10^{-4}	-	-
L11	0.902×10^{-4}	-	-

Table S7. Key photovoltaic parameters calculated from the J_{ph}-V_{eff} curves of L6-L11 blended with PM6 based devices.

Samples	**J_{sat} (mA cm^{-2})**	**J_{ph}^{b} (mA cm^{-2})**	**J_{ph}^{c} (mA cm^{-2})**	**J_{ph}^{b}/ J_{sat} (%)**	**J_{ph}^{c}/ J_{sat} (%)**
PM6: L6	26.651	24.948	21.595	93.61	81.03
PM6: L7	25.896	25.004	21.833	96.56	84.31
PM6: L8	25.696	24.862	21.668	98.18	84.40
PM6: L9	27.196	26.415	22.744	97.13	83.63
PM6: L10	24.987	24.533	21.09	96.75	83.50
PM6: L11	24.684	23.686	20.116	95.96	81.49

[a] The J_{ph} under condition of V_{eff} = 3.0 V; [b] The J_{ph} under short circuit condition; [c] The J_{ph} under maximum power output condition.

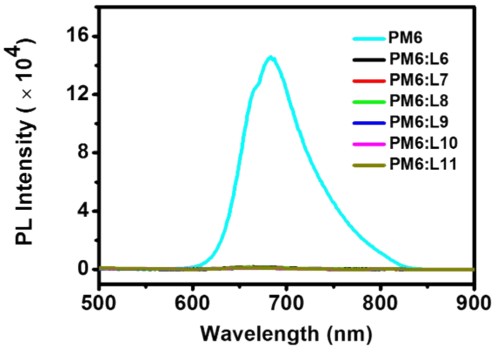

Figure S4. Fluorescence spectrum of donor PM6 quenching by acceptors L6-L11.

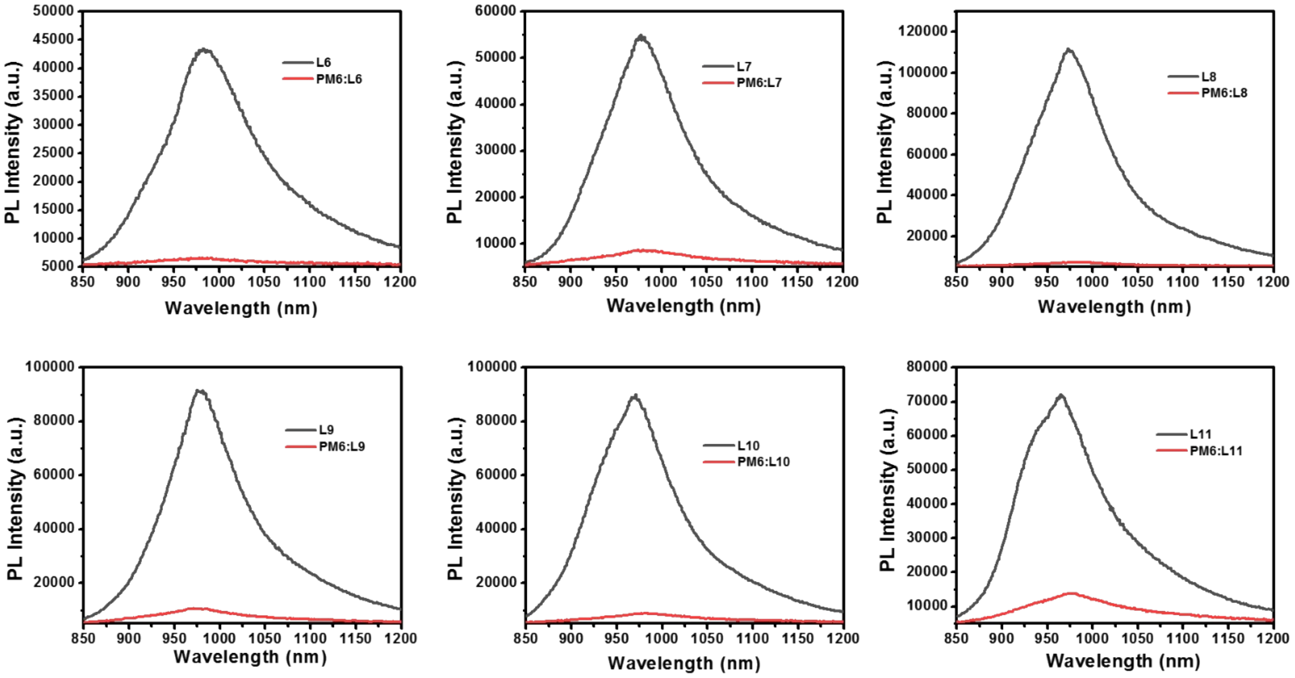

Figure S5. Fluorescence quenching profiles of acceptors L6-L11 when blended with donor PM6.

Table S8. Fluorescence quenching efficiency of PM6 and six acceptors.

D:A	**Fluorescence quenching efficiency of PM6 (%)**	**Fluorescence quenching efficiency of acceptor (%)**
PM6:L6	98.76	85.15
PM6:L7	99.07	85.10
PM6:L8	99.31	93.39
PM6:L9	99.24	88.44
PM6:L10	99.22	90.24
PM6:L11	99.08	82.00

Table S9. Contact angles, surface tensions (γ) and interaction parameters (χ).

Surface	θ_{water}(°)	θ_{EG}(°)	γ (mN m^{-1})	χ^{D-A}
PM6	105.32	86.4	38.46	-
L6	106.08	84.62	39.40	0.006
L7	96.49	81.05	48.28	0.558
L8	98.87	74.16	49.50	0.695

L9	104.56	80.98	43.39	0.149
L10	104.07	82.27	43.10	0.132
L11	104.12	81.71	42.66	0.109

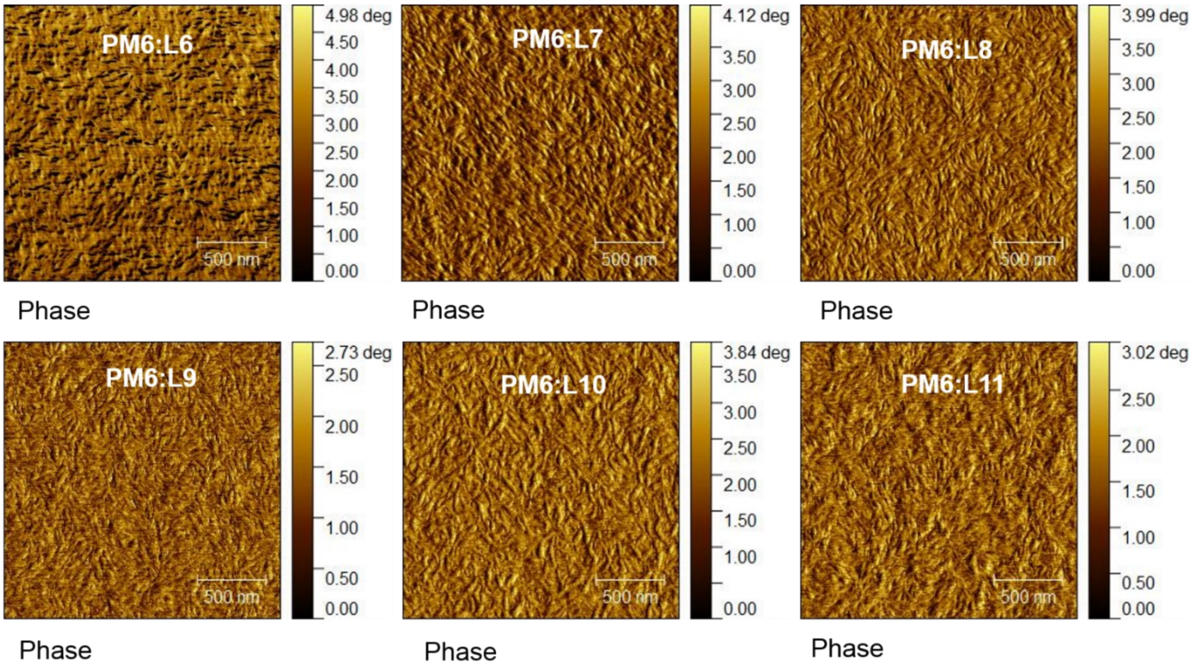

Figure S6. The phase profiles of L6-L11 blended with PM6.

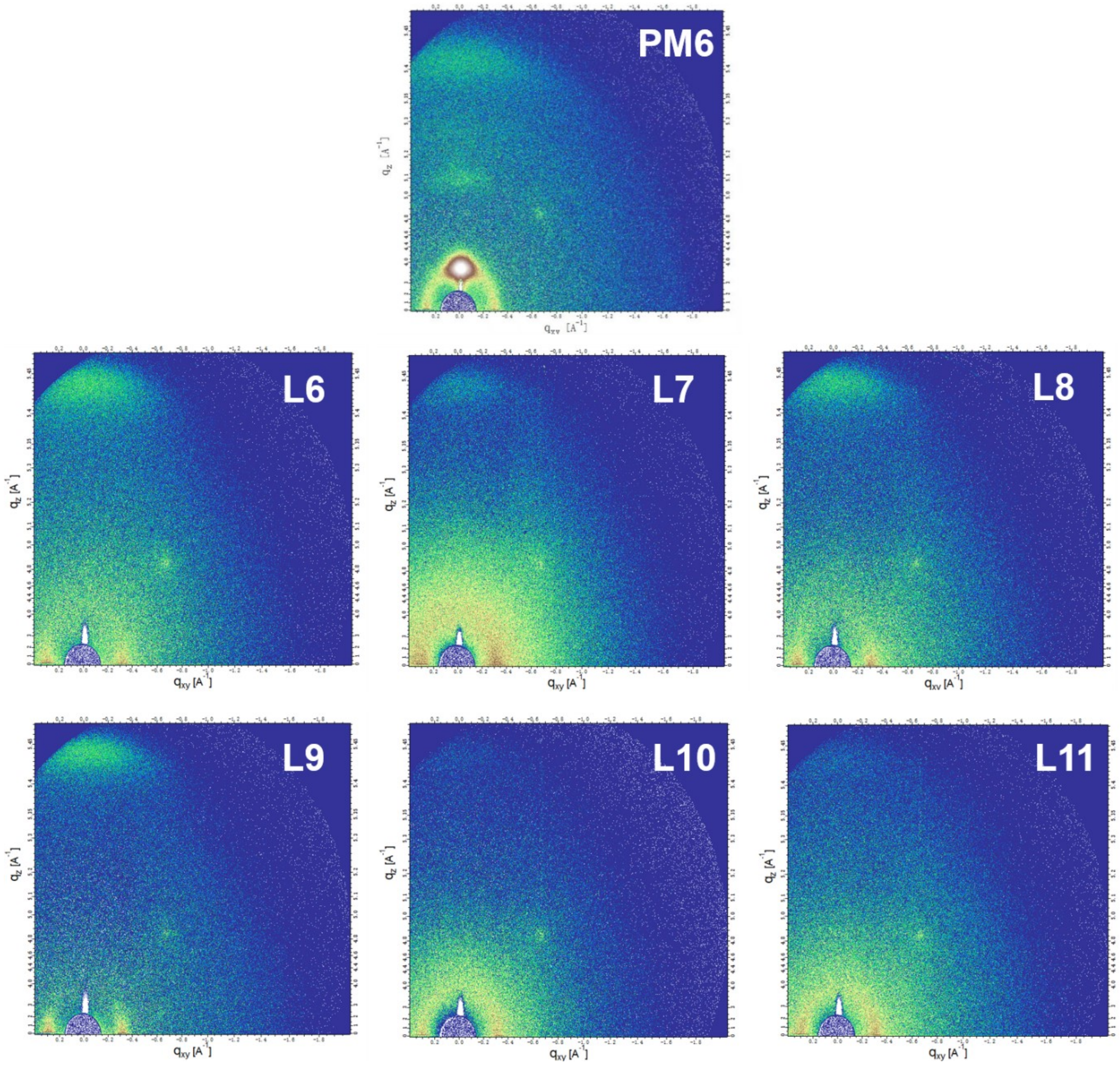

Figure S7. Two-dimensional GIWAXS patterns of pure PM6 and acceptor films under optimal conditions.

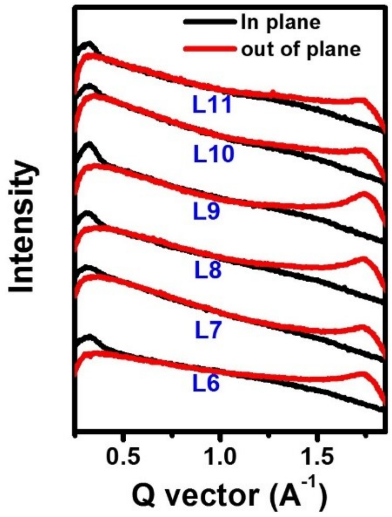

Figure S8. GIWAXS 1D line-cut profiles of L6-L11 neat films.

Table S10. The diffraction vector (q) values of diffraction peaks and crystal correlation length (CCL) in neat and blend films.

Film	q (010, Å^{-1})	d-spacing^{a} (010, Å^{-1})	CCL^{b} (010, Å^{-1})	q (100, Å^{-1})	d-spacing^{a} (100, Å^{-1})	CCL^{b} (100, Å^{-1})
PM6:L6	1.725	3.642	40.392	0.311	20.20	94.247
PM6:L7	1.725	3.642	41.888	0.310	20.27	115.40
PM6:L8	1.716	3.661	42.200	0.311	20.20	117.81
PM6:L9	1.711	3.672	38.732	0.308	20.40	134.64
PM6:L10	1.721	3.650	40.977	0.303	20.74	161.56
PM6:L11	1.707	3.681	41.560	0.301	20.87	171.36
PM6	1.64	3.83	22.35	0.298	21.08	87.00
L6	1.743	3.604	57.119	0.319	19.70	76.420
L7	1.727	3.638	67.319	0.32	19.63	53.347
L8	1.738	3.615	68.131	0.313	20.07	54.373
L9	1.743	3.604	63.537	0.321	19.57	68.131
L10	1.722	3.649	85.680	0.323	19.45	61.466
L11	1.727	3.638	94.247	0.314	20.01	50.944

a) Calculated from the equation: d-spacing = 2π/q. b) Obtained from the Scherrer equation: CCL = 2 πK/FWHM, where FWHM is the full-width at half-maximum and K is a shape factor (K = 0.9 here).

Synthetic Details

Synthesis of compound L6: To a 100 ml round bottom flask, compound D6 (120 mg, 0.1 mmol), 5,6-dichloro-1,1-dicyanomethylene-3-indanone (IC-2Cl) (105.6 mg, 0.403 mmol), chloroform (30 ml) were added under argon protection and stirred for a while when pyridine (1 ml) was added. The mixture was kept stirring at 65 °C for 24 hours. After removal of chloroform of reaction mixture under reduced pressure, 100 ml methanol was added and the precipitate was collected by filtration. The residue was purified by column chromatography on silica gel using a mixture solvent as eluent (petroleum ether/dichloromethane, v/v = 1/1) to give a dark solid (98 mg, 59%).

^{1}H NMR (400 MHz, CDCl$_3$): δ 8.87 (s, 1H), 8.83 (s, 1H), 8.75 (s, 1H), 8.66 (s, 1H), 7.90-7.85 (d, 2H), 7.70-7.69 (d, 2H), 7.51 (s, 1H), 7.32-7.30 (m, 5H), 7.16-7.10 (m, 12H), 3.81-3.77 (d, 2H), 2.61-2.56 (q, 8H), 1.62-1.56 (m, 8H), 1.36-1.27 (br, 24H), 1.14-1.06 (m, 3H), 0.89-0.85 (br, 10H), 0.69 (t, 3H).

^{13}C NMR (100 MHz, CDCl$_3$): δ 186.13, 185.90, 161.30, 158.46, 158.17, 157.96, 156.61, 150.93, 147.60, 142.82, 142.40, 140.95, 140.56, 140.22, 139.64, 139.33, 139.16, 138.96, 138.78, 138.69, 138.61, 136.88, 136.74, 136.01, 135.42, 128.80, 128.76, 128.46, 127.71, 126.97, 126.61, 125.09, 124.77, 120.84, 120.43, 118.89, 117.61, 115.09, 114.89, 114.30, 67.24, 62.93, 62.64, 48.41, 35.56, 35.53, 32.26, 31.71, 31.68, 31.30, 29.10, 22.59, 22.57, 19.87, 14.09, 13.51.

MALDI-TOF: $C_{98}H_{87}Cl_4N_5O_2S_3$ (M$^+$), calcd, 1604.4780, found, 1604.4765.

Synthesis of compound L7: Compound L7 (TPIC-4Cl) was synthesized according to our published paper.[S1]

Synthesis of compound L8: The synthesis route of L8 is similar to the synthesis of L6 by replacing compound D6 with compound D8. The mixture was purified by column chromatography on silica gel with petroleum ether/dichloromethane (3:2, v/v) as an eluent to give a dark solid (130.0 mg, 78%).

^{1}H NMR (400 MHz, CDCl$_3$): δ 8.87 (s, 1H), 8.80 (s, 1H), 8.74 (s, 1H), 8.66 (s, 1H), 7.89-7.86 (d, 2H), 7.68-7.67 (d, 2H), 7.50 (s, 1H), 7.32-7.29 (m, 5H), 7.15-7.10 (m, 12H), 3.69-3.67(d, 2H), 2.61-2.56 (q, 8H), 1.63-1.56 (m, 8H), 1.35-1.25 (br, 28H), 1.10-0.99 (m, 5H), 0.89-0.63 (br, 26H).

^{13}C NMR (100 MHz, CDCl$_3$): δ 186.12, 185.85, 161.35, 158.83, 158.47, 158.15, 157.93, 156.55, 151.21, 148.68, 142.81, 142.39, 140.93, 140.50, 140.22, 139.64, 139.32, 139.15, 138.96, 138.81, 138.72, 138.67, 138.60, 136.93, 136.89, 136.58, 136.01, 135.43, 128.83, 128.75, 127.70, 126.96, 126.60, 125.08, 124.77, 120.80, 120.43, 118.86, 117.51, 115.02, 114.90, 114.30, 69.39, 67.37, 62.91, 62.88, 53.22, 37.62, 35.55, 31.70, 31.68, 31.37, 31.31, 30.80, 30.54, 29.71, 29.57, 29.13, 29.10, 28.83, 26.61, 22.94, 22.59, 14.09, 13.95.

MALDI-TOF: $C_{106}H_{103}Cl_4N_5O_2S_3$ (M$^+$), calcd,1716.6032, found, 1716.6032.

Synthesis of compound L9: The synthesis route of L9 is similar to the synthesis of L6 by replacing compound D6 with compound D9. The mixture was purified by column chromatography on silica gel with petroleum ether/dichloromethane (3:2, v/v) as an eluent to give a dark solid (134 mg, 75.5%).

^{1}H NMR (400 MHz, CDCl$_3$): δ 8.87 (s, 1H), 8.81 (s, 1H), 8.74 (s, 1H), 8.66 (s, 1H), 7.89-7.86 (d, 2H), 7.68-7.67 (d, 2H), 7.50 (s, 1H), 7.31-7.29 (m, 5H), 7.14-7.09 (m, 12H), 3.68-3.66 (d, 2H), 2.61-2.56 (q, 8H), 1.61-1.57 (m, 8H), 1.34-1.25 (br, 34H), 1.13-1.10 (br, 9H), 0.89-0.83 (br, 21H), 0.63 (t, 3H).

^{13}C NMR (100 MHz, CDCl$_3$): δ 186.13, 161.34, 158.82, 158.16, 157.93, 156.55, 151.19, 148.66, 142.80, 142.40, 140.93, 140.49, 140.22, 139.64, 139.32, 138.97, 138.71, 138.68, 138.60, 136.93, 136.89, 136.58, 136.02, 135.43, 128.83, 128.75, 127.70, 126.96, 126.61, 125.09, 124.78, 120.81, 120.42, 114.30, 69.39, 67.36, 62.91, 62.87, 35.55, 31.90, 31.70, 31.68, 31.38, 31.31, 30.88, 30.82, 29.90, 29.71, 29.58, 29.44, 29.27, 29.15, 29.10, 26.65, 26.62, 22.69, 22.59, 14.12, 14.09.

MALDI-TOF: $C_{110}H_{111}Cl_4N_5O_2S_3$ (M^+), calcd,1772.6658, found, 1772.6655.

Synthesis of compound L10: The synthesis route of L10 is similar to the synthesis of L6 by replacing compound D6 with compound D10. The mixture was purified by column chromatography on silica gel with petroleum ether/dichloromethane (3:2, v/v) as an eluent to give a dark solid (140 mg, 76.6%).

^{1}H NMR (400 MHz, CDCl$_3$): ^{1}H NMR (400 MHz, CDCl$_3$): δ 8.87 (s, 1H), 8.80 (s, 1H), 8.74 (s, 1H), 8.66 (s, 1H), 7.89-7.86 (d, 2H), 7.68-7.67 (d, 2H), 7.50 (s, 1H), 7.31-7.29 (m, 5H), 7.14-7.09 (m, 12H), 3.68-3.66 (d, 2H), 2.61-2.56(q, 8H), 1.61-1.58 (m, 8H), 1.35-1.17 (br, 41H), 1.12-1.10 (br, 10H), 0.89-0.84 (br, 21H), 0.64 (t, 3H).

^{13}C NMR (100 MHz, CDCl$_3$): δ 186.13, 185.83, 161.35, 158.82, 158.46, 158.16, 157.93, 156.56, 151.20, 148.66, 142.80, 142.39, 140.93, 140.50, 140.22, 139.64, 139.32, 139.16, 138.97, 138.79, 138.71, 138.67, 138.61, 136.91, 136.58, 136.02, 135.43, 128.83, 128.75, 127.70, 126.96, 126.60, 125.09, 124.77, 120.80, 120.43, 118.87, 117.51, 115.01, 114.89, 114.30, 69.39, 67.36, 62.92, 62.87, 37.61, 35.56, 31.94, 31.91, 31.71, 31.39, 31.31, 30.84, 29.91, 29.68, 29.65, 29.51, 29.44, 29.39, 29.28, 29.16, 29.10, 26.64, 22.70, 22.59, 14.12, 14.10, 1.02.

MALDI-TOF: $C_{114}H_{119}Cl_4N_5O_2S_3$ (M^+), calcd,1828.7284, found, 1828.7285.

Synthesis of compound L11: The synthesis route of L11 is similar to the synthesis of L6 by replacing compound D6 with compound D11. The mixture was purified by column chromatography on silica gel with petroleum ether/dichloromethane (3:2, v/v) as an eluent to give a dark solid (137 mg, 72.8%).

^{1}H NMR (400 MHz, CDCl$_3$): δ 8.80 (s, 1H), 8.75 (s, 1H), 8.68 (s, 1H), 8.61 (s, 1H), 7.82-7.80 (d, 2H), 7.61-7.59 (d, 2H), 7.42 (s, 1H), 7.23-7.21 (m, 5H), 7.07-7.04 (m, 12H), 3.61-3.53 (d, 2H), 2.54-2.48 (q, 8H), 1.54-1.47 (m, 8H), 1.23-1.15 (br, 50H), 1.03-0.93 (br, 10H), 0.80-0.78 (br, 20H), 0.57-0.55 (m, 3H).

^{13}C NMR (100 MHz, CDCl$_3$): δ 186.13, 185.83, 161.32, 158.84, 158.51, 158.18, 157.98, 156.60, 151.16, 148.65, 142.82, 142.41, 140.95, 140.55, 140.24, 139.67, 139.34, 139.17, 139.01, 138.74, 138.61, 136.95, 136.60, 136.05, 135.44, 128.84, 128.76, 127.72, 126.99, 126.63, 125.10, 124.79, 120.86, 120.44, 118.87, 117.52, 115.01, 114.88, 114.31, 69.44, 67.42, 62.91, 53.28, 37.58, 35.56, 31.94, 31.71, 31.36, 31.29, 30.87, 29.91, 29.75, 29.70, 29.66, 29.51, 29.39, 29.15, 29.09, 26.64, 22.69, 22.58, 14.10, 14.07.

MALDI-TOF: $C_{118}H_{127}Cl_4N_5O_2S_3$(M$^+$), calcd,1884.7910, found,1884.7901.

Copy of characterization data.

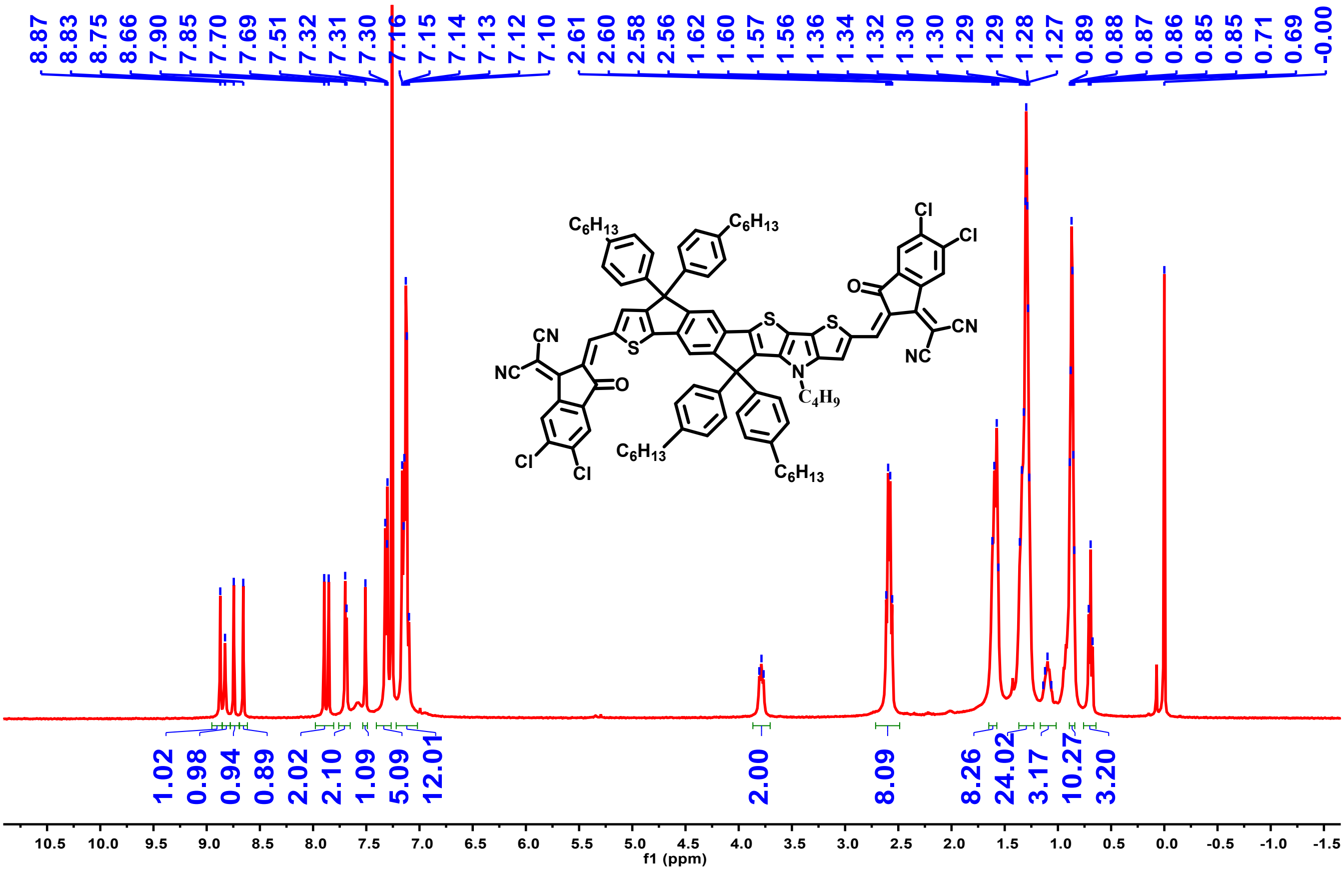

Figure S9. ^{1}H NMR spectrum of compound **L6**.

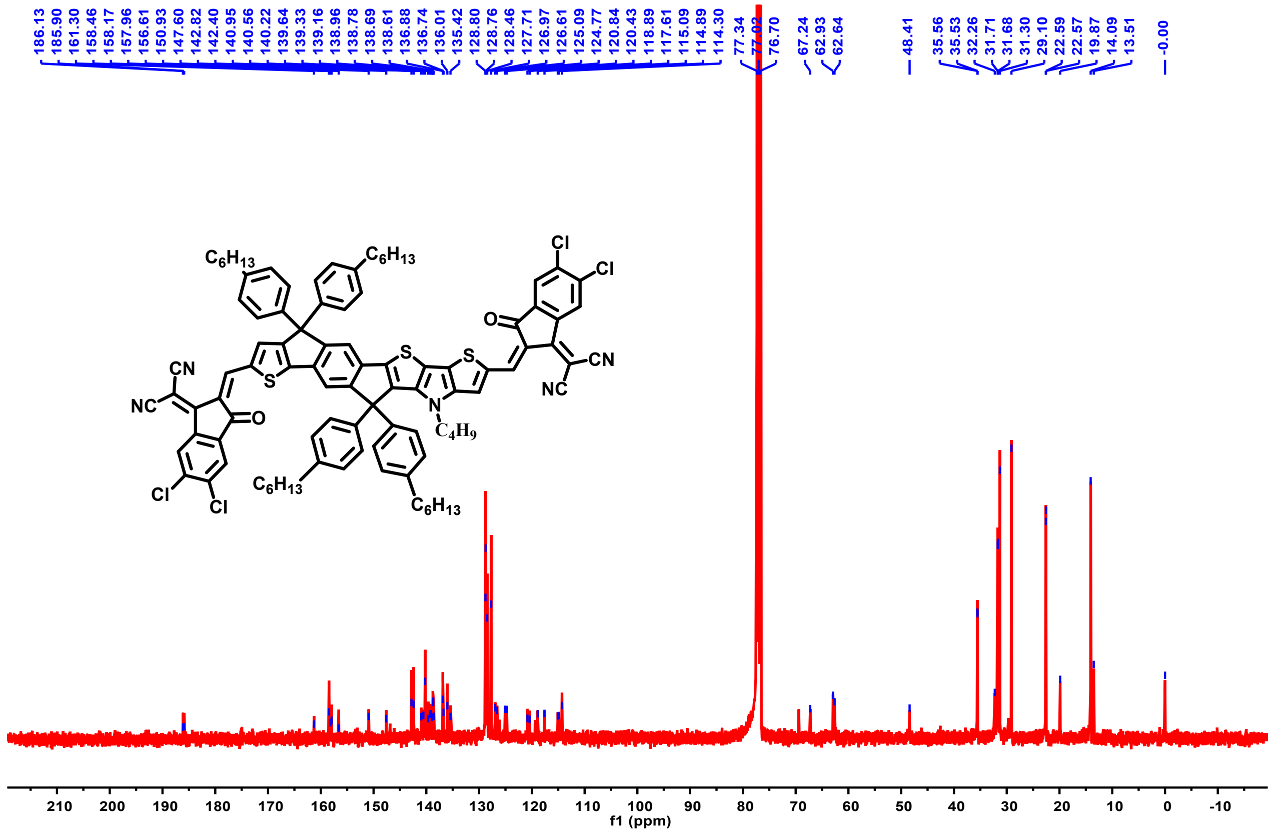

Figure S10. ^{13} C NMR spectrum of compound **L6**.

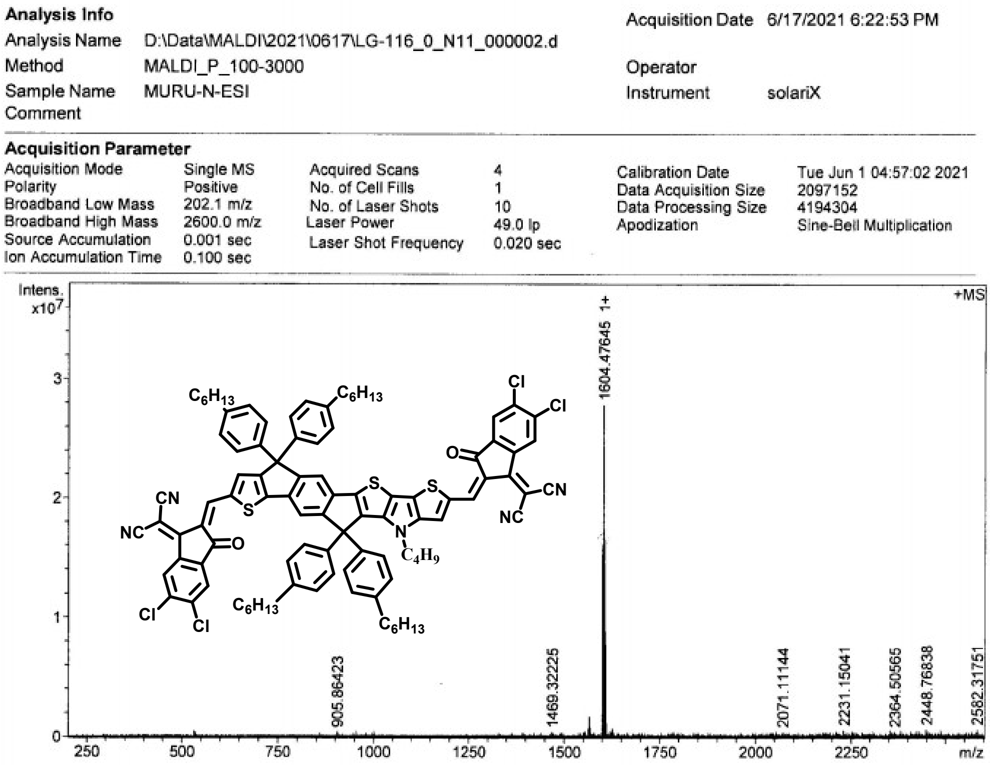

Analysis Info

Analysis Name D:\Data\MALDI\2021\0617\LG-116_0_N11_000002.d
Method MALDI_P_100-3000
Sample Name MURU-N-ESI
Comment

Acquisition Date 6/17/2021 6:22:53 PM

Operator
Instrument solariX

Acquisition Parameter

Acquisition Mode Single MS
Polarity Positive
Broadband Low Mass 202.1 m/z
Broadband High Mass 2600.0 m/z
Source Accumulation 0.001 sec
Ion Accumulation Time 0.100 sec

Acquired Scans 4
No. of Cell Fills 1
No. of Laser Shots 10
Laser Power 49.0 lp
Laser Shot Frequency 0.020 sec

Calibration Date Tue Jun 1 04:57:02 2021
Data Acquisition Size 2097152
Data Processing Size 4194304
Apodization Sine-Bell Multiplication

Figure S11. HRMS profile of compound **L6**.

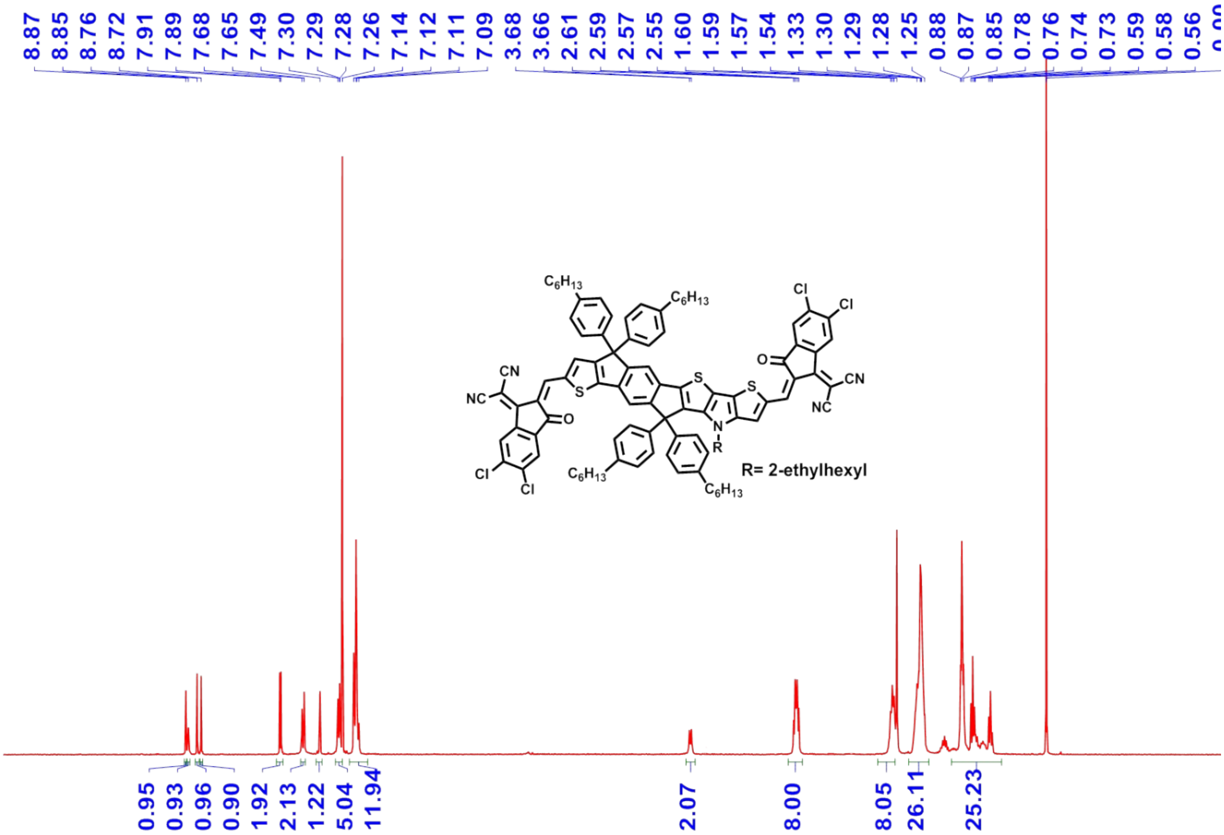

Figure S12. ^{1}H NMR spectrum of compound **L7**.

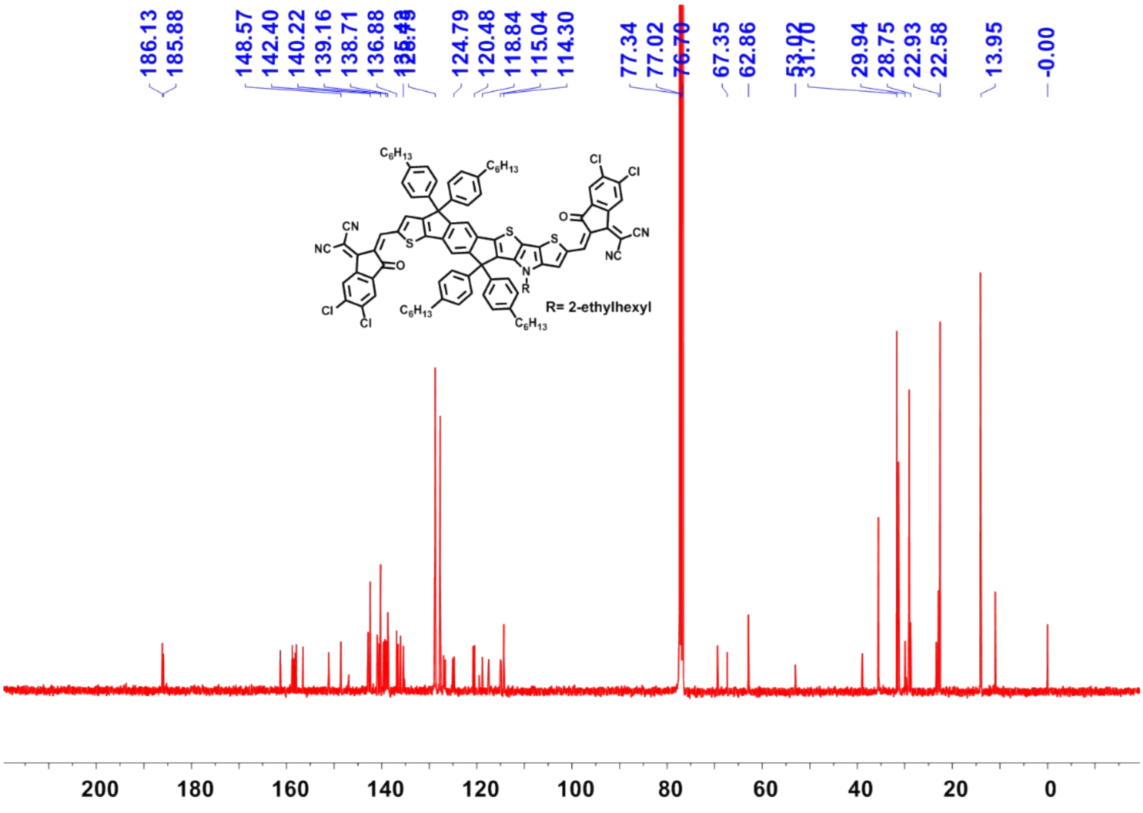

Figure S13. ^{13} C NMR spectrum of compound **L7**.

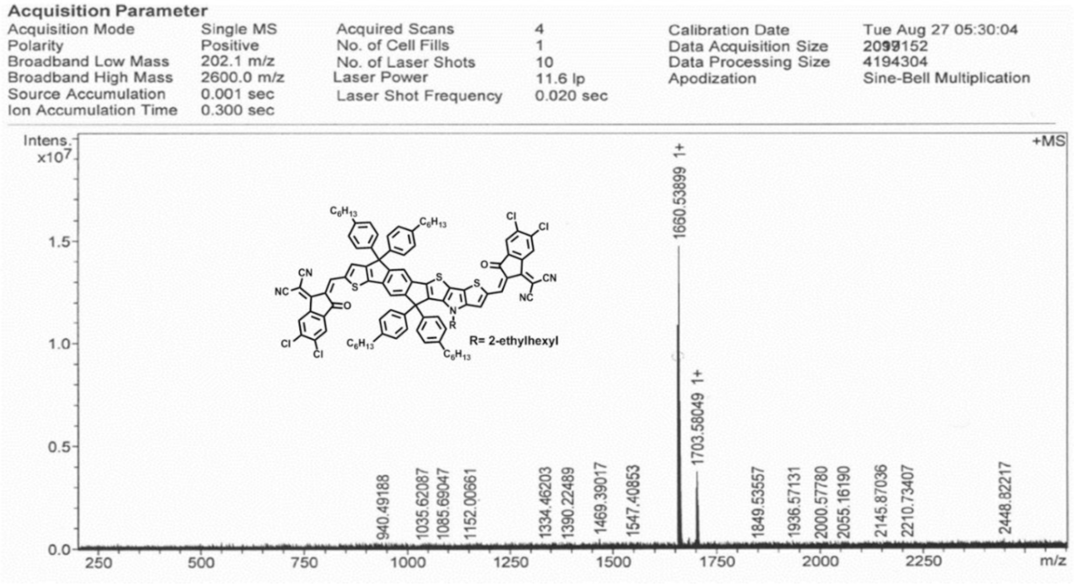

Acquisition Parameter

Acquisition Mode	Single MS	Acquired Scans	4	Calibration Date	Tue Aug 27 05:30:04
Polarity	Positive	No. of Cell Fills	1	Data Acquisition Size	2097152
Broadband Low Mass	202.1 m/z	No. of Laser Shots	10	Data Processing Size	4194304
Broadband High Mass	2600.0 m/z	Laser Power	11.6 lp	Apodization	Sine-Bell Multiplication
Source Accumulation	0.001 sec	Laser Shot Frequency	0.020 sec		
Ion Accumulation Time	0.300 sec				

Figure S14. HRMS profile of compound **L7**.

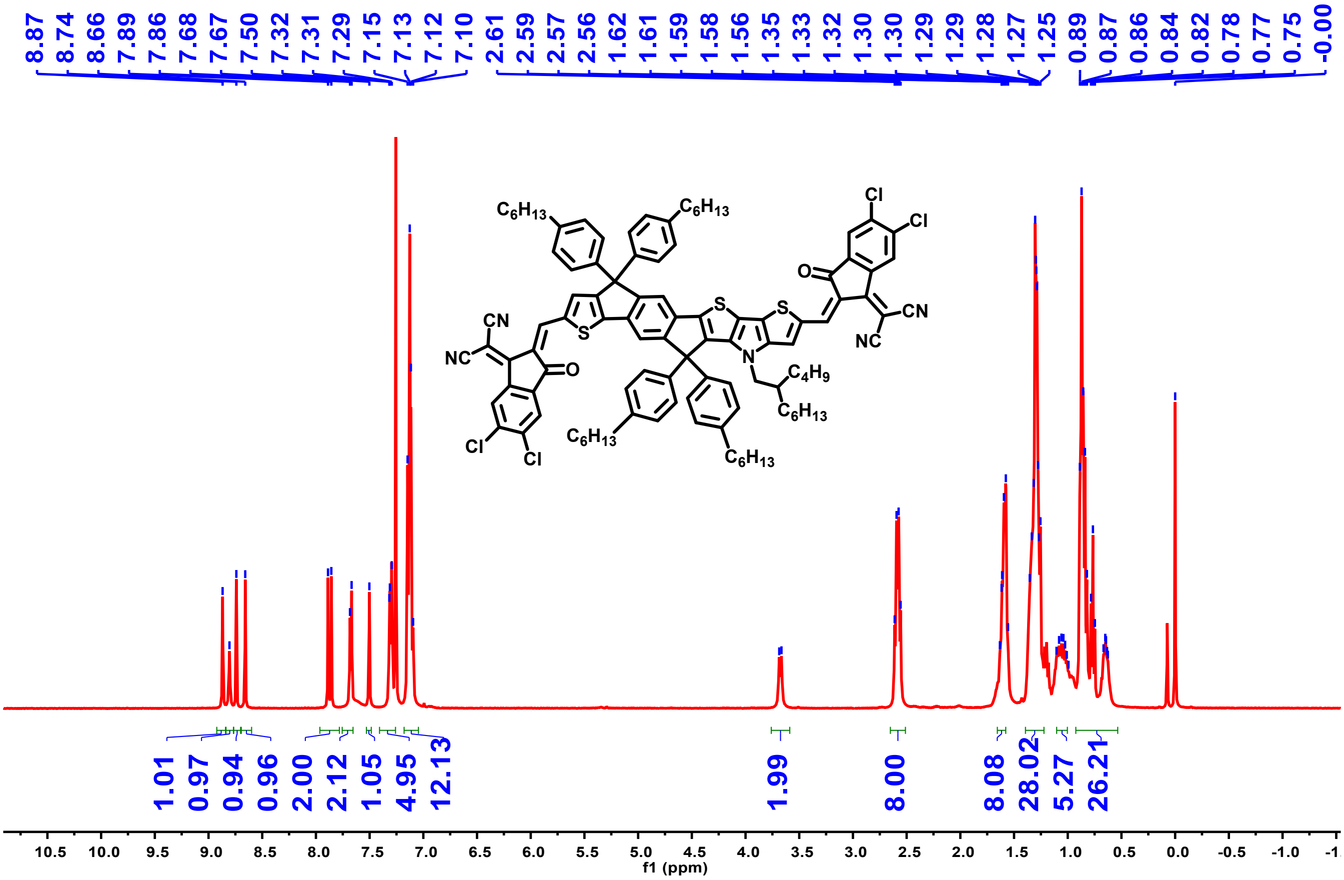

Figure S15. ^{1}H NMR spectrum of compound **L8**.

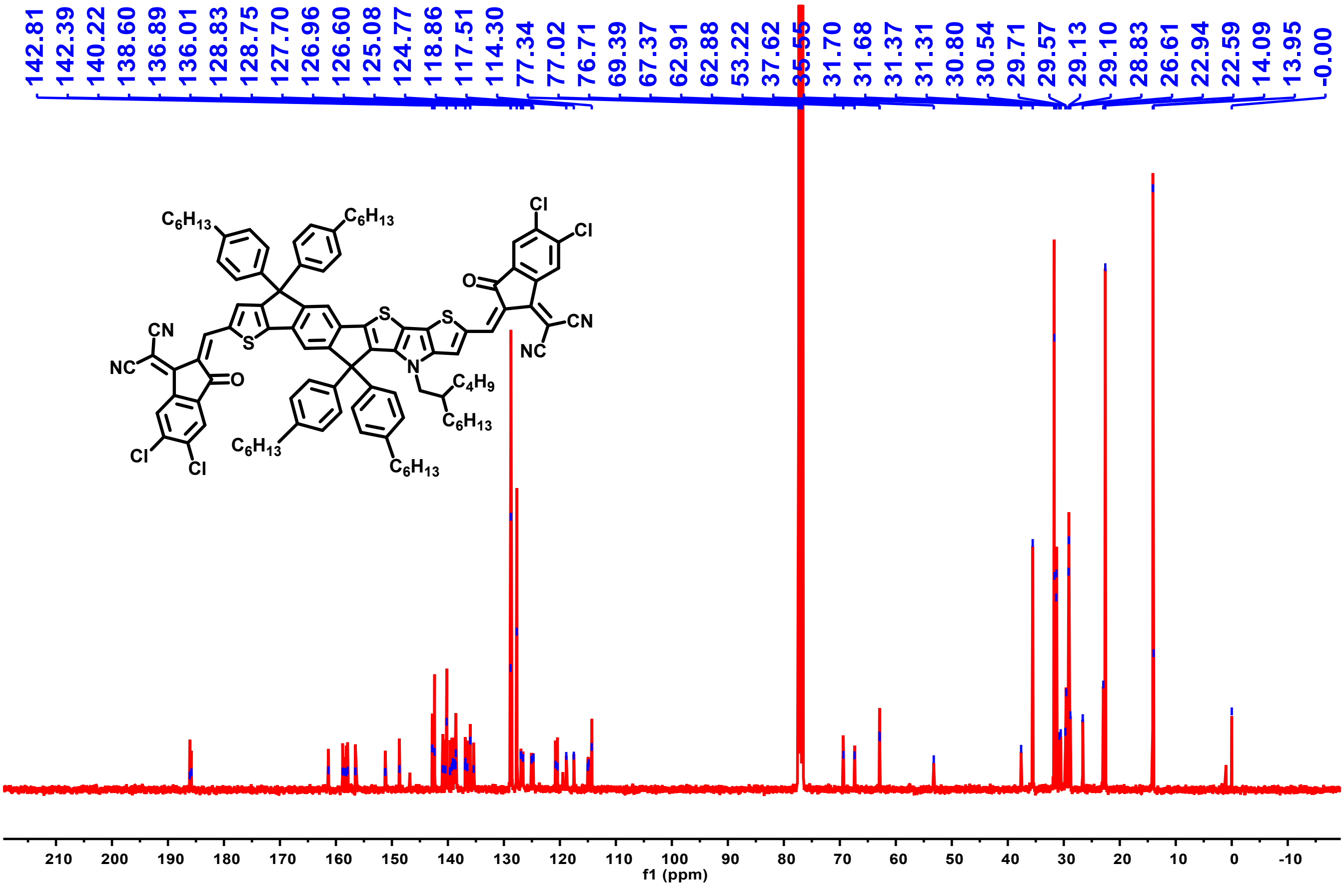

Figure S16. ^{13}C NMR spectrum of compound **L8**.

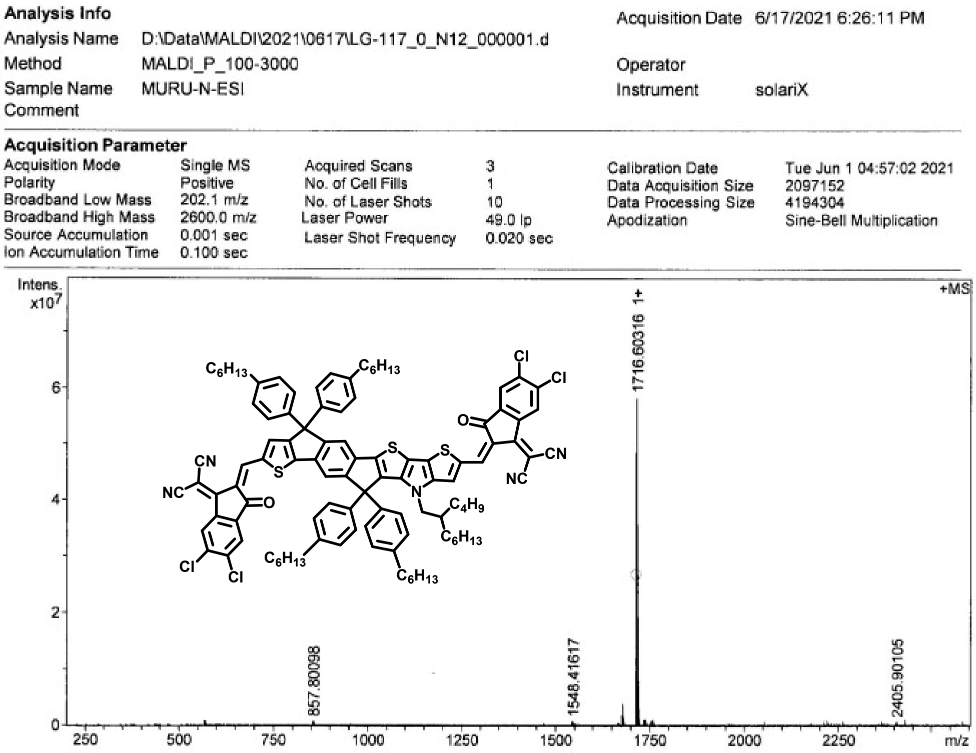

Analysis Info

Analysis Name D:\Data\MALDI\2021\0617\LG-117_0_N12_000001.d
Method MALDI_P_100-3000
Sample Name MURU-N-ESI
Comment

Acquisition Date 6/17/2021 6:26:11 PM
Operator
Instrument solariX

Acquisition Parameter

Acquisition Mode Single MS
Polarity Positive
Broadband Low Mass 202.1 m/z
Broadband High Mass 2600.0 m/z
Source Accumulation 0.001 sec
Ion Accumulation Time 0.100 sec

Acquired Scans 3
No. of Cell Fills 1
No. of Laser Shots 10
Laser Power 49.0 lp
Laser Shot Frequency 0.020 sec

Calibration Date Tue Jun 1 04:57:02 2021
Data Acquisition Size 2097152
Data Processing Size 4194304
Apodization Sine-Bell Multiplication

Figure S17. HRMS profile of compound **L8**.

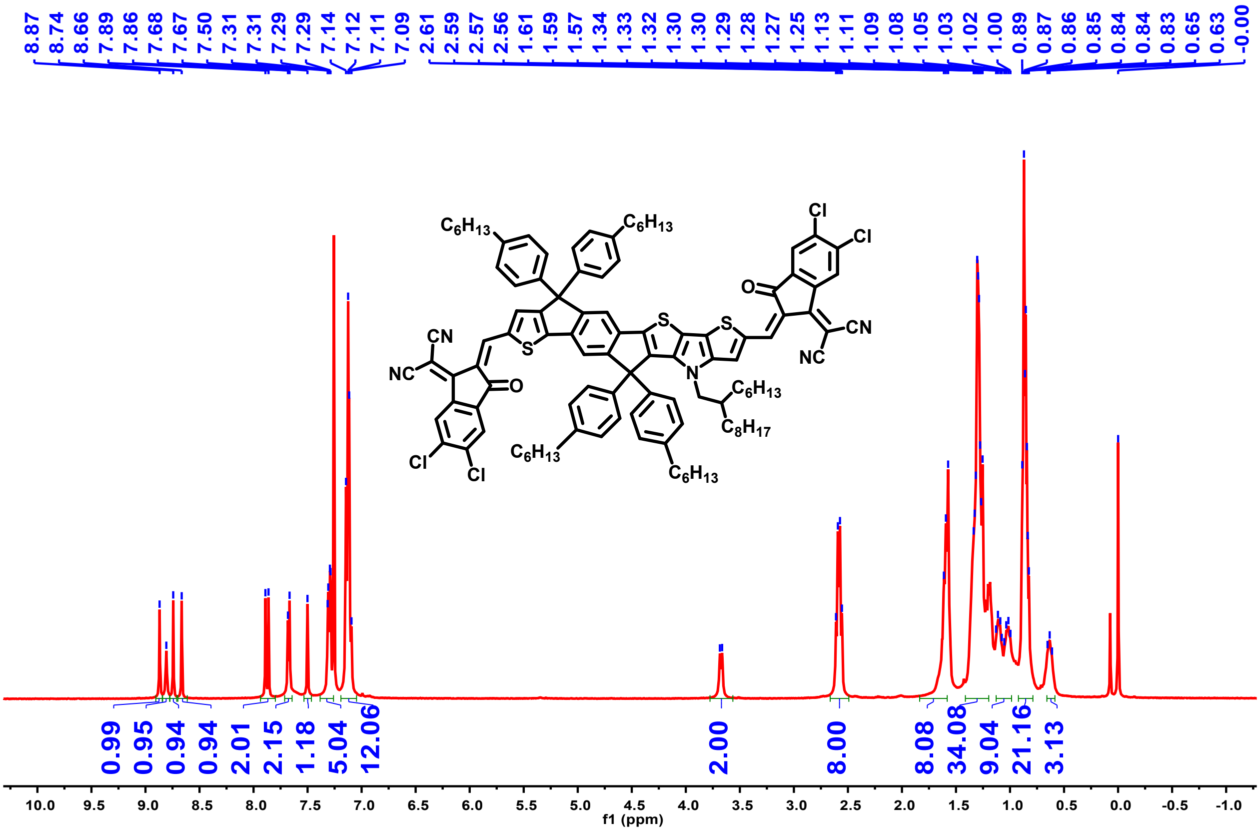

Figure S18. ^{1}H NMR spectrum of compound **L9**.

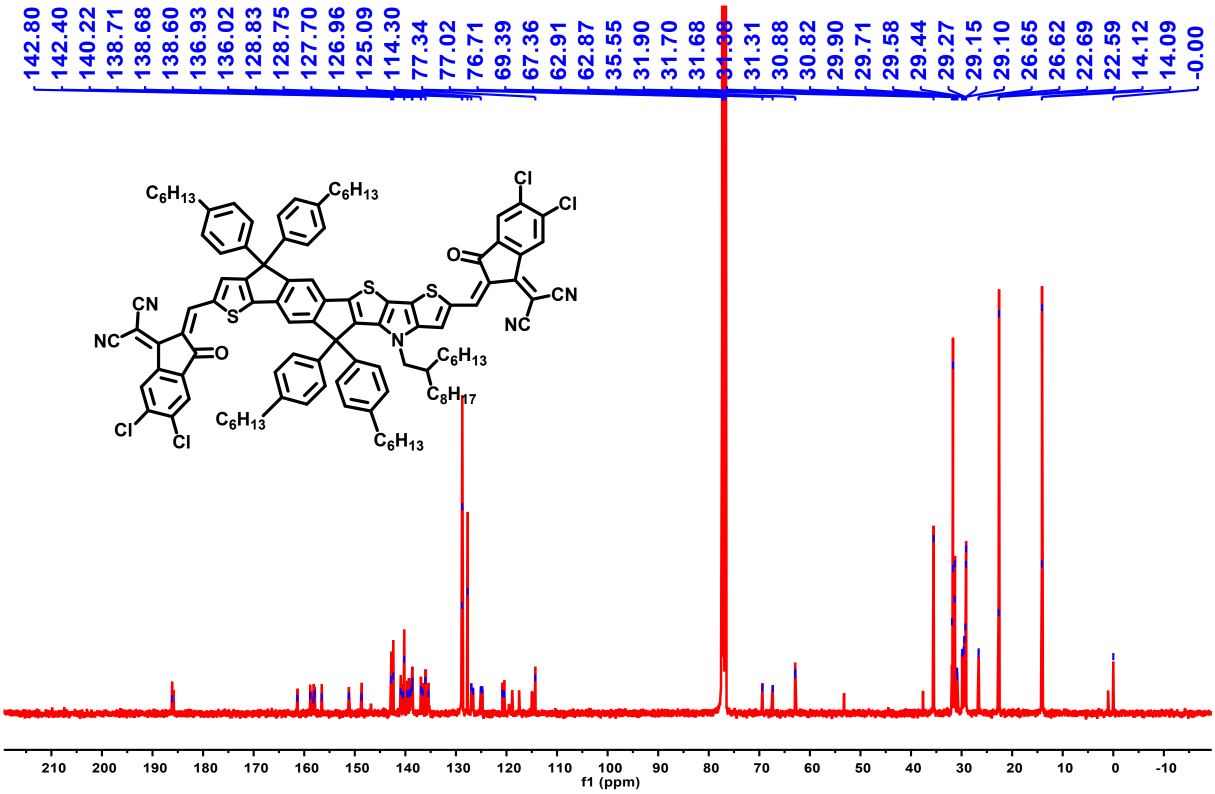

Figure S19. ^{13}C NMR spectrum of compound **L9**.

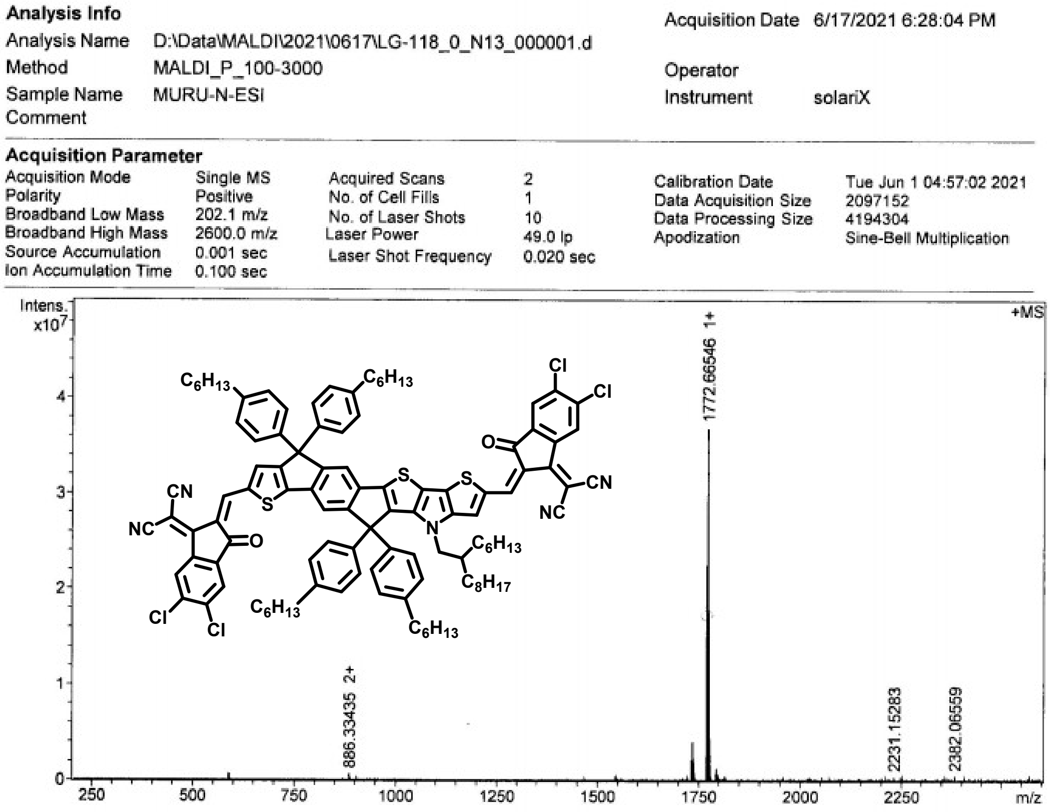

Analysis Info

Analysis Name	D:\Data\MALDI\2021\0617\LG-118_0_N13_000001.d	Acquisition Date	6/17/2021 6:28:04 PM
Method	MALDI_P_100-3000	Operator	
Sample Name	MURU-N-ESI	Instrument	solariX
Comment			

Acquisition Parameter

Acquisition Mode	Single MS	Acquired Scans	2	Calibration Date	Tue Jun 1 04:57:02 2021
Polarity	Positive	No. of Cell Fills	1	Data Acquisition Size	2097152
Broadband Low Mass	202.1 m/z	No. of Laser Shots	10	Data Processing Size	4194304
Broadband High Mass	2600.0 m/z	Laser Power	49.0 lp	Apodization	Sine-Bell Multiplication
Source Accumulation	0.001 sec	Laser Shot Frequency	0.020 sec		
Ion Accumulation Time	0.100 sec				

Figure S20. HRMS profile of compound **L9**.

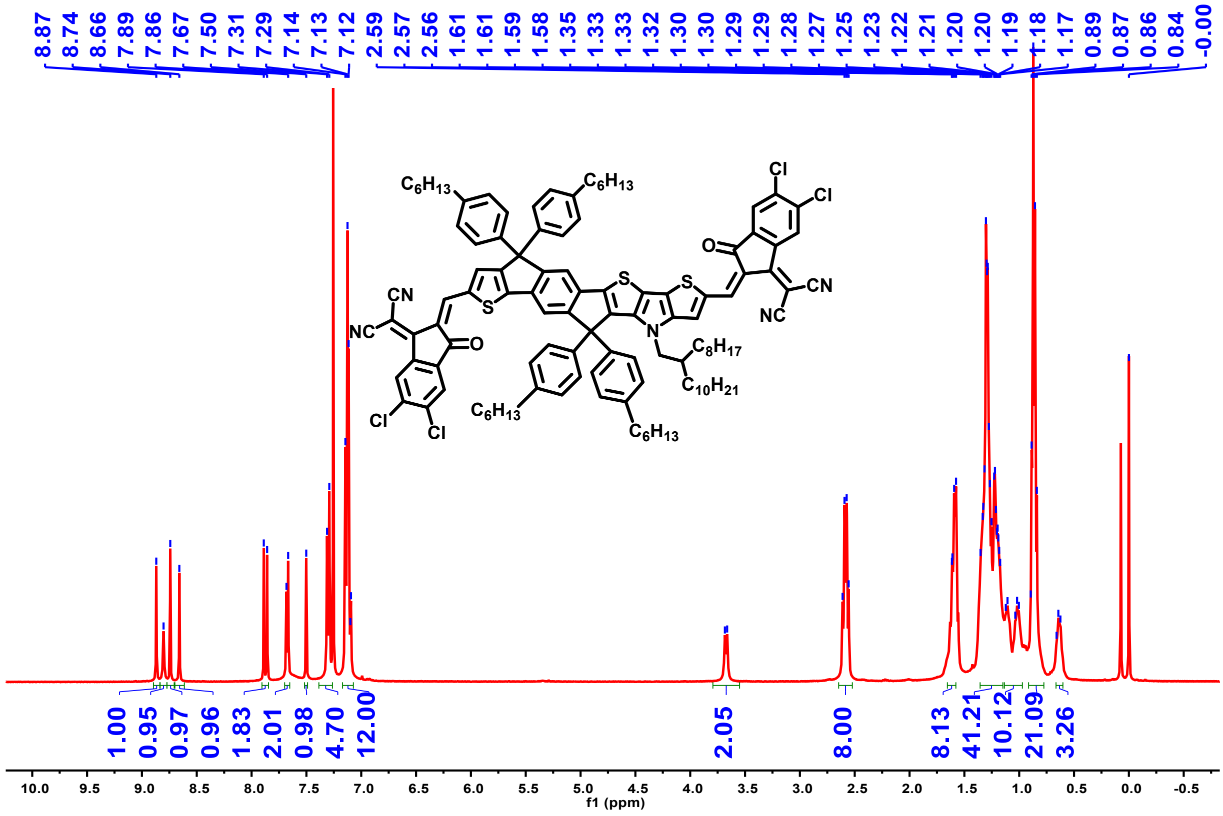

Figure S21. ^{1}H NMR spectrum of compound **L10**.

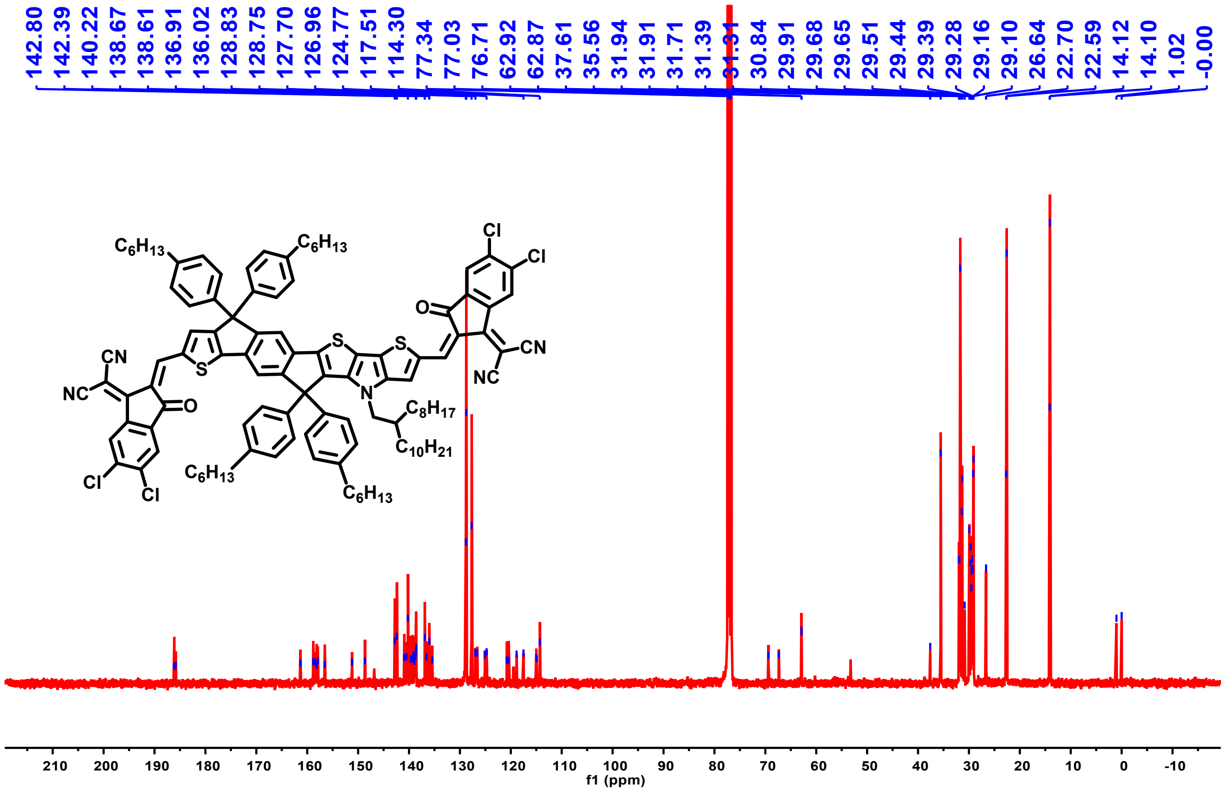

Figure S22. ^{13} C NMR spectrum of compound **L10**.

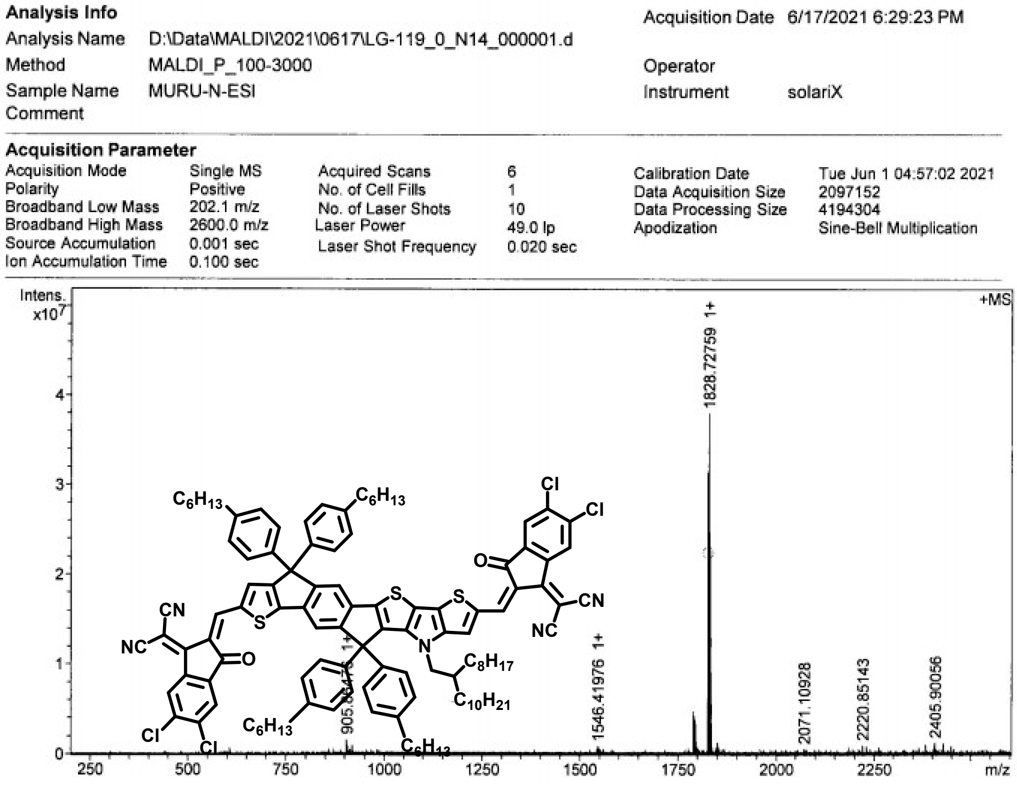

Analysis Info

Analysis Name	D:\Data\MALDI\2021\0617\LG-119_0_N14_000001.d	Acquisition Date	6/17/2021 6:29:23 PM
Method	MALDI_P_100-3000	Operator	
Sample Name	MURU-N-ESI	Instrument	solariX
Comment			

Acquisition Parameter

Acquisition Mode	Single MS	Acquired Scans	6	Calibration Date	Tue Jun 1 04:57:02 2021
Polarity	Positive	No. of Cell Fills	1	Data Acquisition Size	2097152
Broadband Low Mass	202.1 m/z	No. of Laser Shots	10	Data Processing Size	4194304
Broadband High Mass	2600.0 m/z	Laser Power	49.0 lp	Apodization	Sine-Bell Multiplication
Source Accumulation	0.001 sec	Laser Shot Frequency	0.020 sec		
Ion Accumulation Time	0.100 sec				

Figure S23. HRMS profile of compound **L10**.

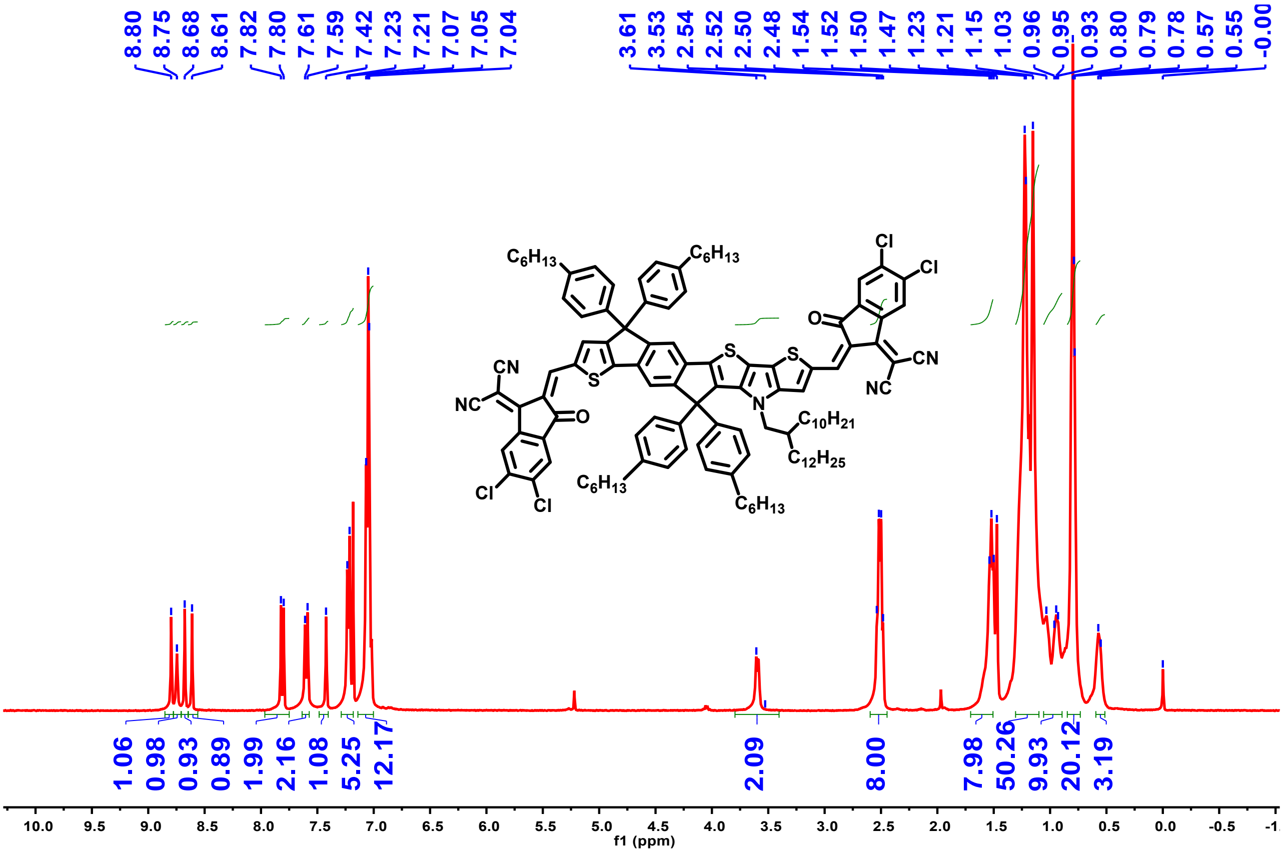

Figure S24. ^{1}H NMR spectrum of compound **L11**.

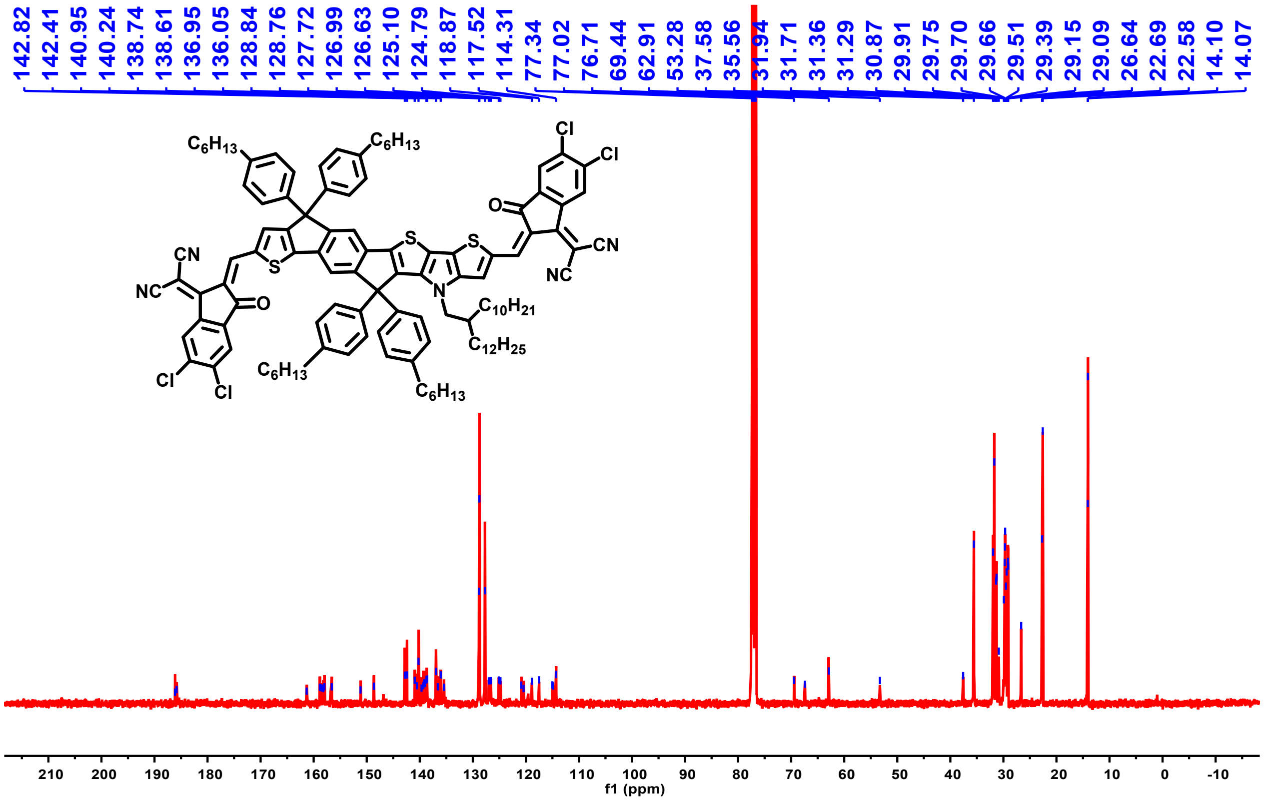

Figure S25. ^{13}C NMR spectrum of compound **L11**.

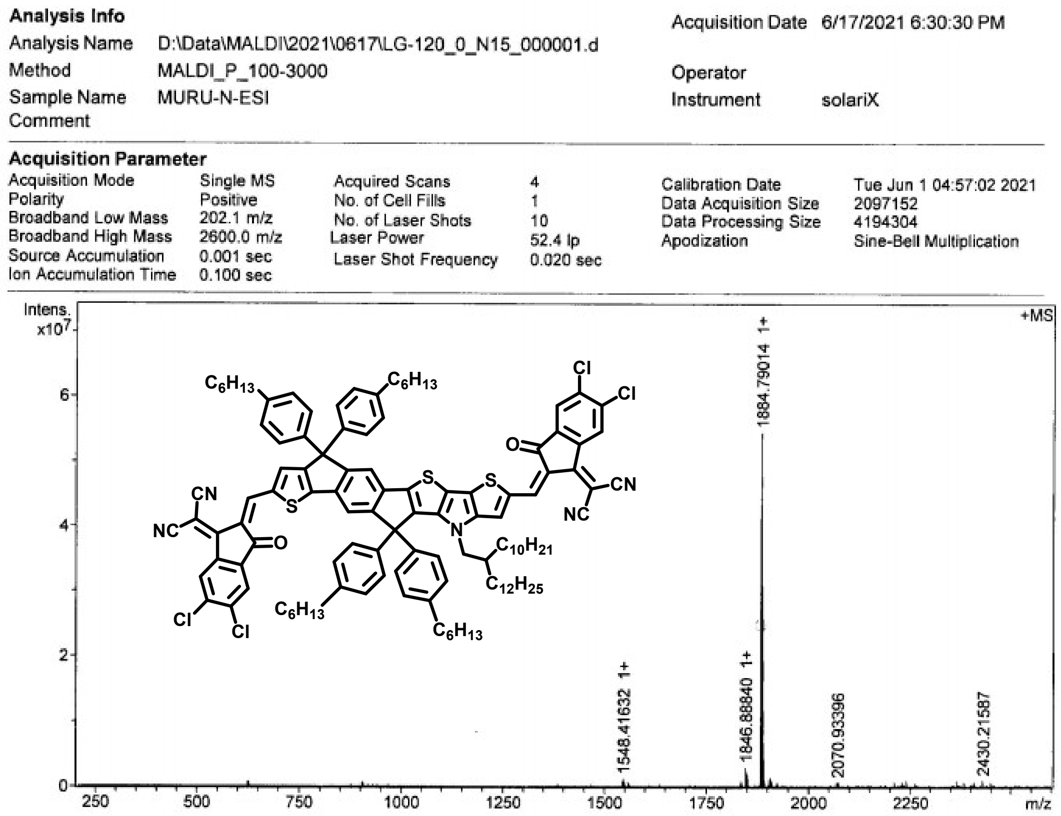

Analysis Info

Analysis Name	D:\Data\MALDI\2021\0617\LG-120_0_N15_000001.d	Acquisition Date	6/17/2021 6:30:30 PM
Method	MALDI_P_100-3000	Operator	
Sample Name	MURU-N-ESI	Instrument	solariX
Comment			

Acquisition Parameter

Acquisition Mode	Single MS	Acquired Scans	4	Calibration Date	Tue Jun 1 04:57:02 2021
Polarity	Positive	No. of Cell Fills	1	Data Acquisition Size	2097152
Broadband Low Mass	202.1 m/z	No. of Laser Shots	10	Data Processing Size	4194304
Broadband High Mass	2600.0 m/z	Laser Power	52.4 lp	Apodization	Sine-Bell Multiplication
Source Accumulation	0.001 sec	Laser Shot Frequency	0.020 sec		
Ion Accumulation Time	0.100 sec				

Figure S26. HRMS profile of compound **L11**.

Reference:

[S1]. G. Li, D. Li, R. Ma, T. Liu, Z. Luo, G. Cui, L. Tong, M. Zhang, Z. Wang, F. Liu, L. Xu, H. Yan, B. Tang, *J. Mater. Chem. A.* 2020, 8, 5927-5935.